Crossflow Instability

Justin Jarmer

Outline

- What is the Crossflow Instability?
- Sensitivity to Surface Roughness
- Transition to Turbulence
- Flight Testing

What is the Crossflow Instability?

Significance

- Occures in swept wing flows
- Swept wing designs came of interest towards the end of WWII
- Delays effects of compressibility
- Can improve longitudinal stability of tailess aircraft

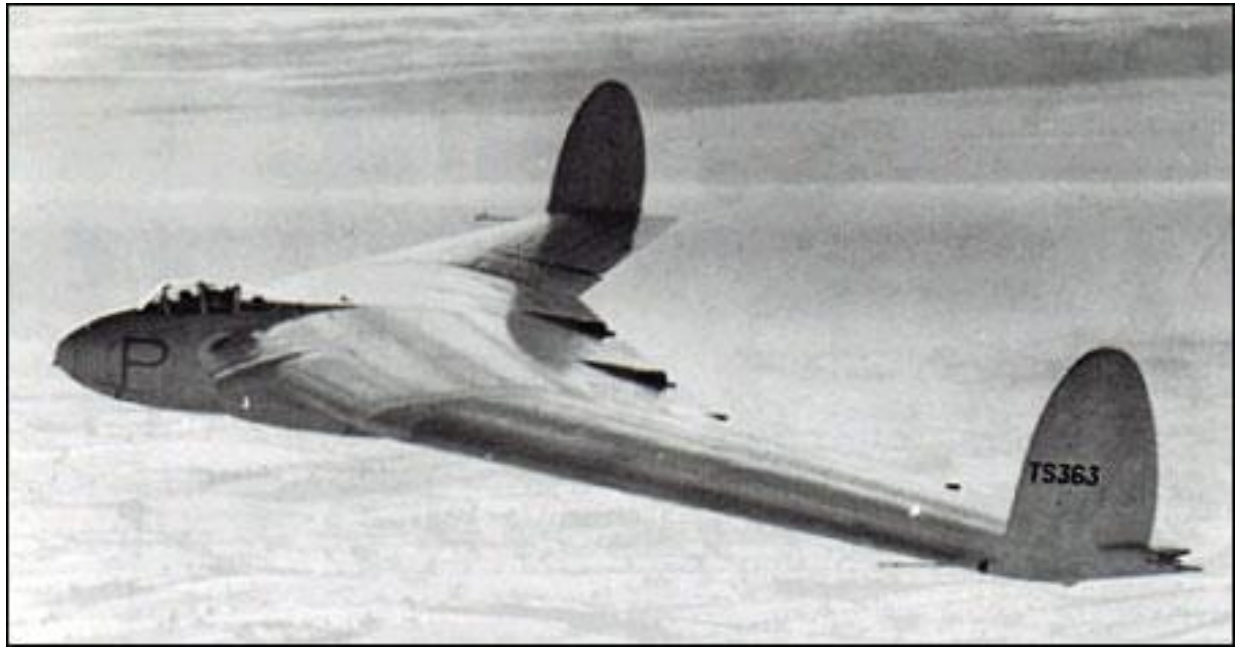

Understanding the Pressure Gradient on an Airfoil

- Favorable pressure gradient until pressure minimum -> then adverse pressure gradient to tailing edge
- Shape of Cp curve changes with angle of attack
- This is pressure measured at the surface of the airfoil
- NACA 64(3) - 618 airfoil

Meersman (2021)

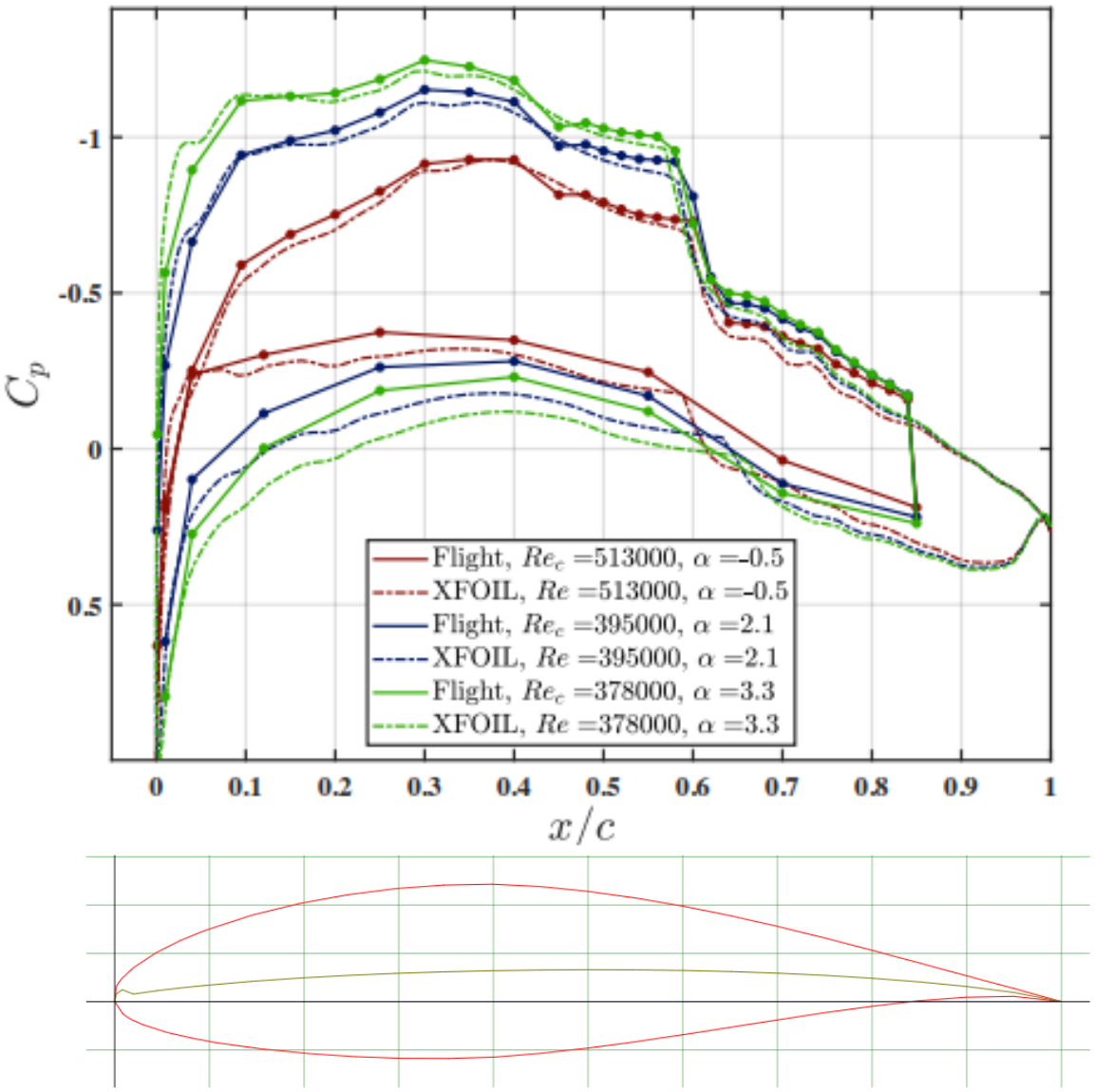

Meersman (2021)

Pressure gradient perpendicular to free stream flow

- When the wing is swept a Pressure gradient perpendicular to free stream flow appears
- Two fluid elements travelling parallel to each other in the free stream will be at different x/c values and as a result will be experiencing different pressures

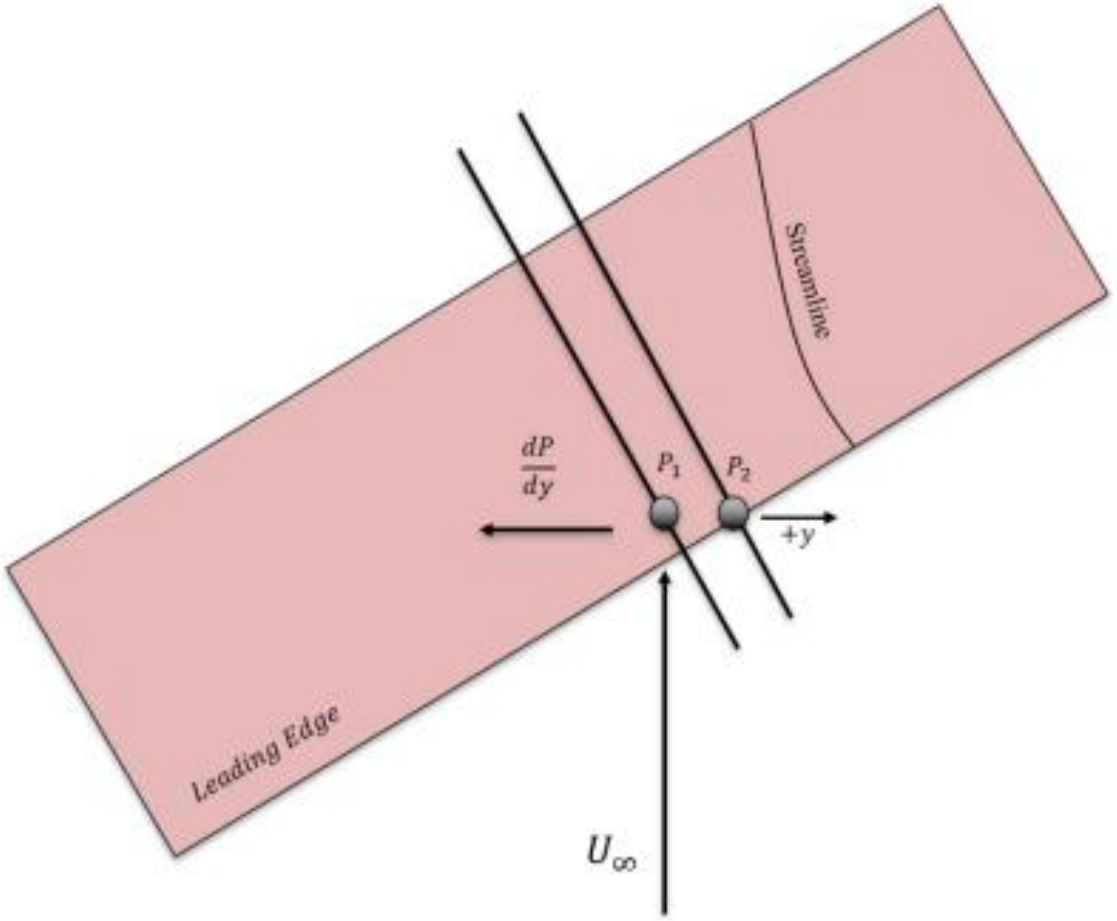

Meersman (2021)

Resulting Flow Profile

- This pressure gradient perpendicular to the free stream flow direction results in a component of the boundary layer flow in the same direction
- Pressure gradient is strongest at the surface of the airfoil, but velocity is forced to zero at the wall
- Results in an inflection point in the flow profile

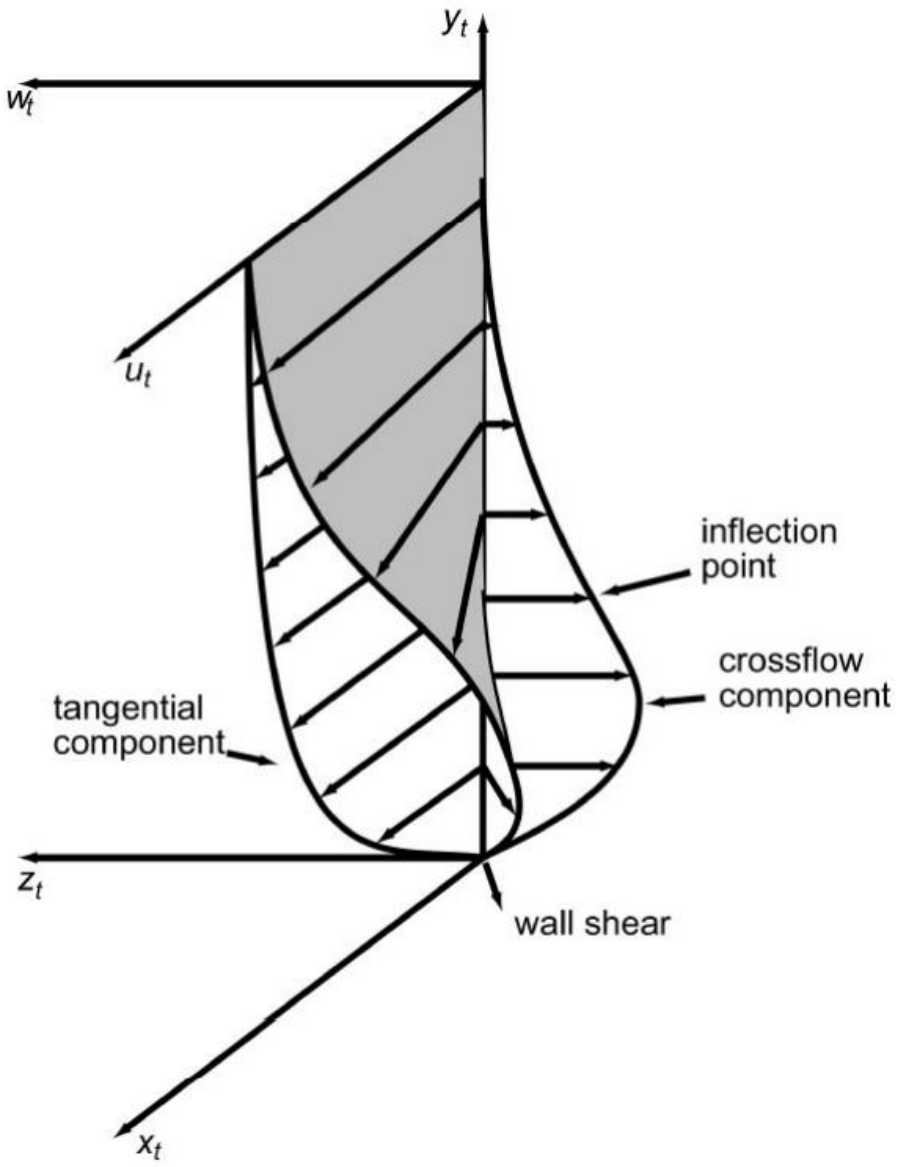

Saric, Reed, White (2003)

Resulting Flow Profile

- Re-adapted from Reed (1988)
- Believed that about 3% of the free stream velocity is typical of the order of magnitude of the crossflow component velocity

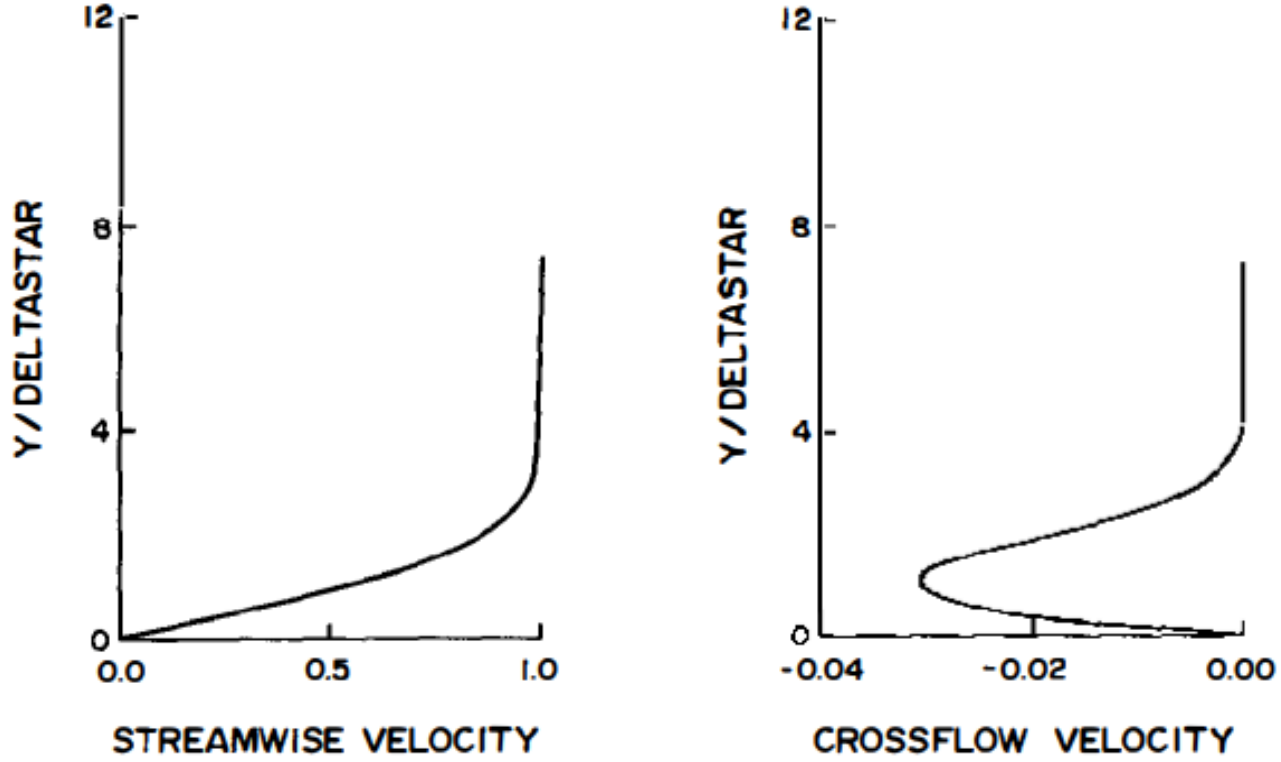

Reed, Saric (1989)

Inviscid Streamline

- This diagram is just a visualization tool and is not based on calculations
- It shows an inboard velocity profile where a favorable pressure gradient is expected and then an outboard flow where we would expect an adverse pressure gradient

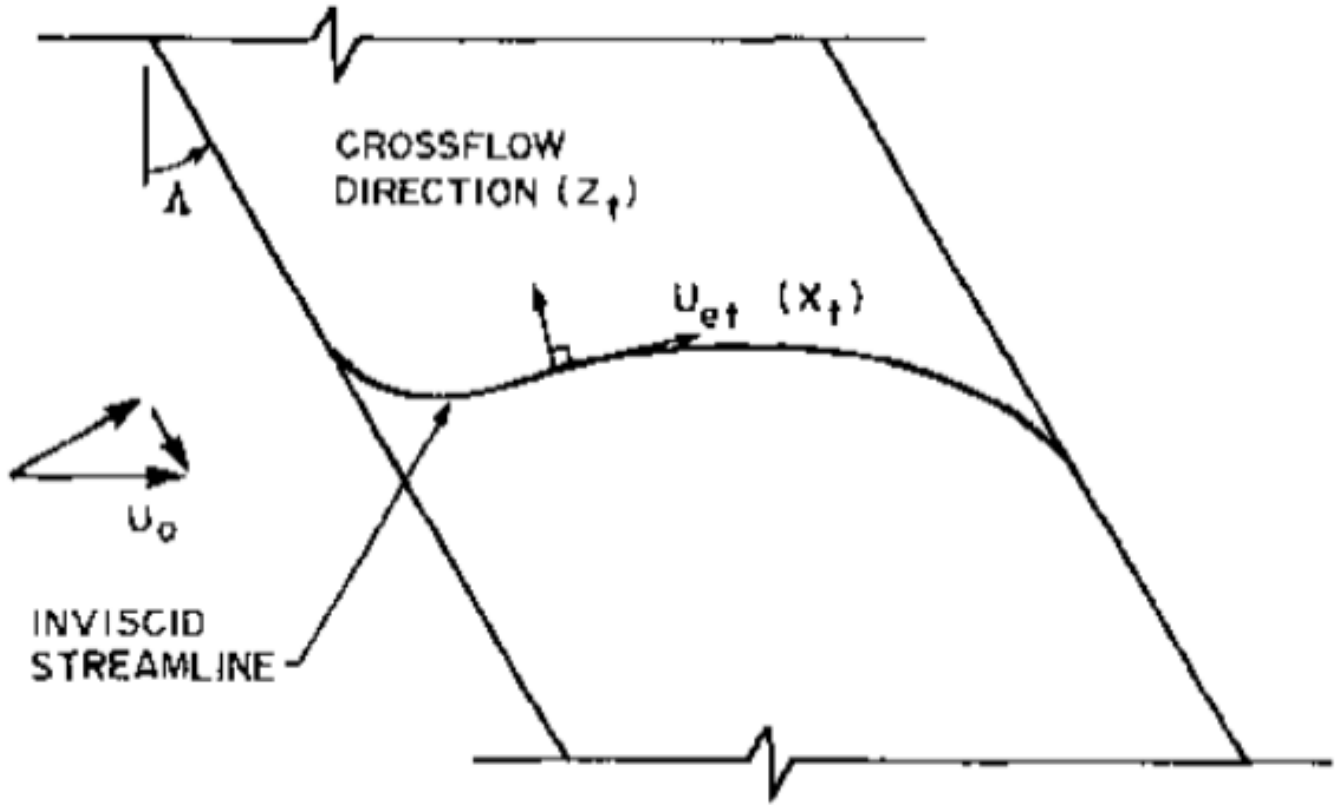

Reed, Saric (1989)

Cross-Flow Vortices

- Co-rotating vortices
- Aligned in freestream direction
- Vortices show periodicity in the spanwise direction
- This periodic structure is typically on the same order of magnitude as the boundary-layer thickness

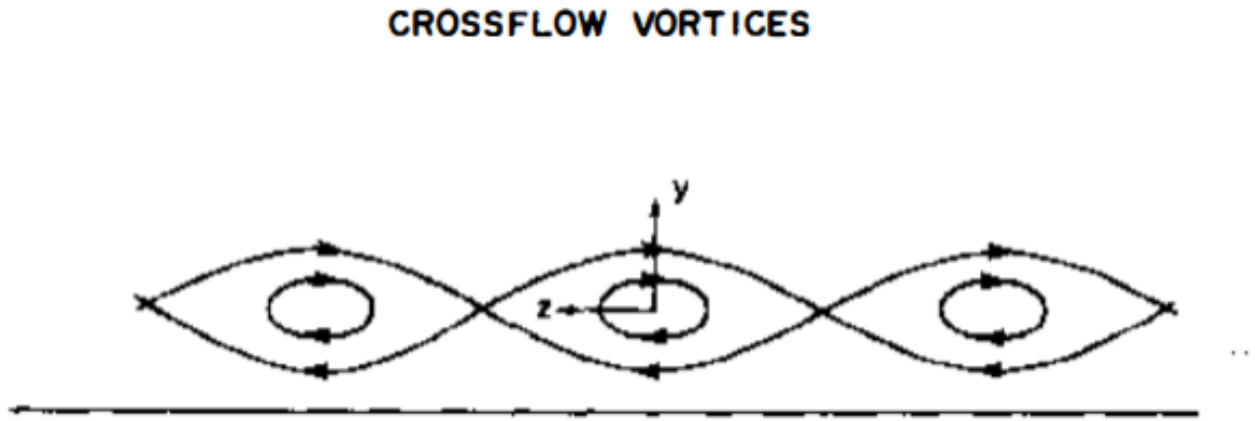

Reed, Saric (1989)

Cross-Flow Vortices

- Depending on the freestream turbulence/vorticity, these CFVs can either be stationary or traveling (in spanwise direction)
- Low turbulence leads to stationary and is expected in most flight testing conditions

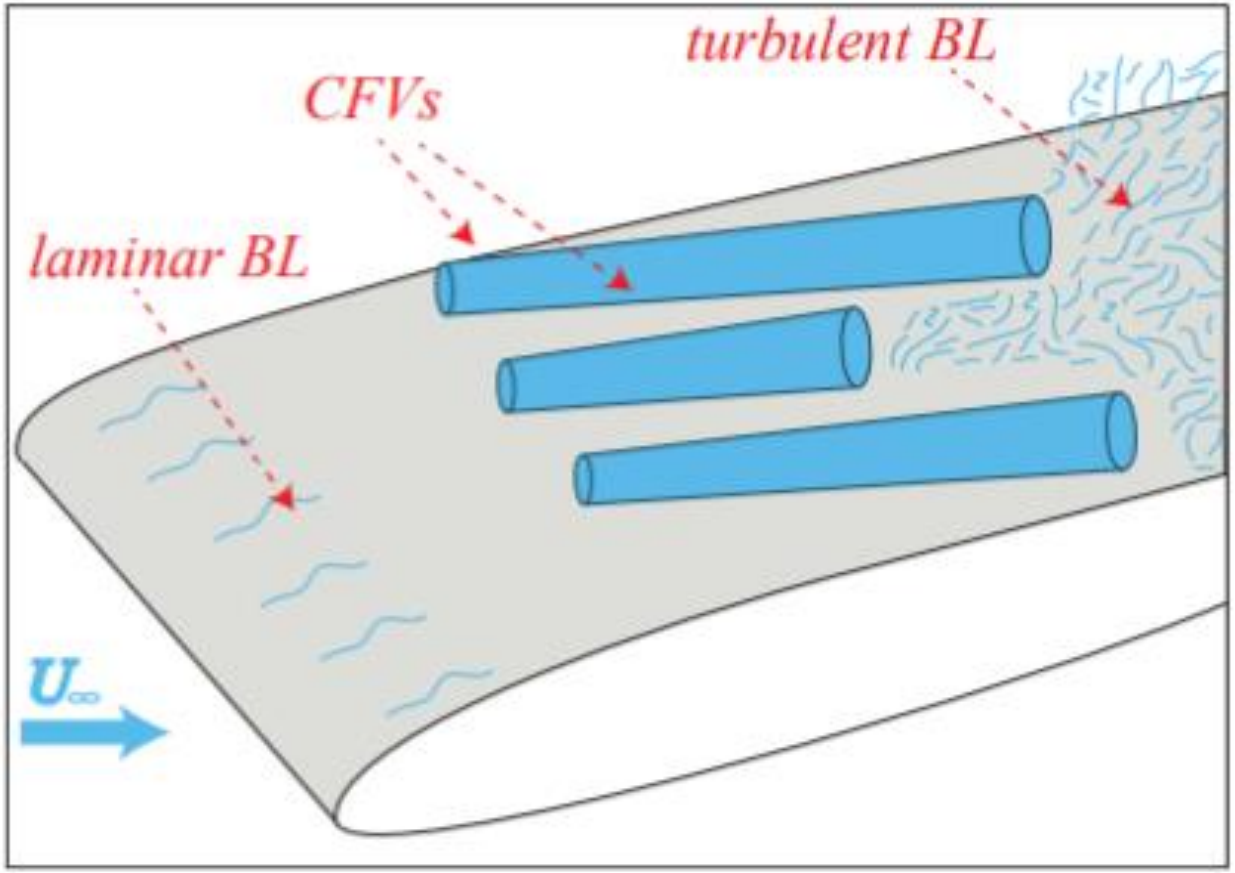

Serpieri (2018)

Cross-Flow Vortices

- Flow is from right to left
- Darker areas show the turbulent regions of the boundary layer
- Transition to turbulence results in a jagged, "saw-tooth" pattern in the location of the beginning of the turbulent BL
- Florescent oil visualization on a 45-degree swept wing at Re = 1.3*10^6
- TU Delft LTT facility

Serpieri (2018)

Stability Equations

- Follows Reibert (1996)
- Begin by assuming a parallel basic state given by:

$$U = U(y), \quad V = 0, \quad W = W(y), \tag{3.4}$$

- Total field quantities include both the basic state plus small, 3-D disturbances written as:

$$u = U + u'(x, y, z, t) \tag{3.5a}$$

$$v = v'(x, y, z, t) \tag{3.5b}$$

$$w = W + w'(x, y, z, t) \tag{3.5c}$$

$$p = P + p'(x, y, z, t) \tag{3.5d}$$

Stability Equations (cont.)

- Previous equations are used in the incompressible Navier-Stokes equations. The basic state is removed, and products of the small disturbance quantities are neglected resulting in the following linear disturbance equations

$$u'_x + v'_y + w'_z = 0 \tag{3.6}$$

$$u'_t + Uu'_x + U_y v' + Wu'_z + p'_x - \nabla^2 u'/R = 0 \tag{3.7}$$

$$v'_t + Uv'_x + Wv'_z + p'_y - \nabla^2 v'/R = 0 \tag{3.8}$$

$$w'_t + Uw'_x + W_y v' + Ww'_z + p'_z - \nabla^2 w'/R = 0 \tag{3.9}$$

- The above equations can be reduced to ordinary differential equations with the introduction of the normal mode:

$$q'(x, y, z, t) = q(y)\, e^{i(\alpha x + \beta z - \omega t)} + C.C., \tag{3.10}$$

- Where q' represents any one of the disturbance quantities and with chordwise wavenumber α (complex), spanwise wavenumber β (complex), and frequency ω.

Stability Equations (cont.)

- Substituting the normal mode into the system of linear disturbance equations and combining them, a single 4th – order equation can be found (Orr-Sommerfeld Eq.):

$$\left\{\left(D^2-k^2\right)^2-iR\left[(\alpha U+\beta W-\omega)\left(D^2-k^2\right)-\alpha\left(D^2U\right)-\beta\left(D^2W\right)\right]\right\}\phi=0, \tag{3.11}$$

- Where $k^2 = \alpha^2 + \beta^2$, D = d/dy, and $\phi = v$ represents the normal-mode amplitude function for the v' disturbance.
- The disturbances must go to zero at the wall and in the free-stream, this gives the BC's

$$\phi(0)=D\phi(0)=0 \quad \text{and} \quad \phi \xrightarrow[y\to\infty]{} 0. \tag{3.12}$$

- This results in a linear, homogeneous system which defines an eigenvalue problem.
- R (Reynolds number) is known, ω is specified, β_i is assumed = 0, and β is often specified when calculating, leaving α_r and α_i to be solved for.

Paths to Turbulence

- There are many paths to turbulence
- This presentation focuses on path A

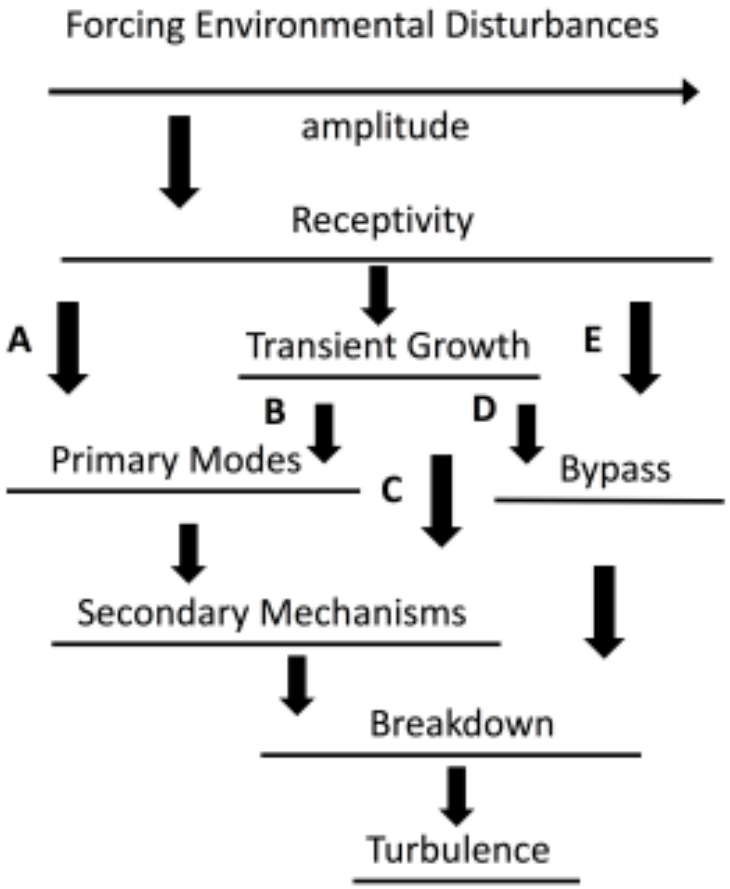

Serpieri (2018)

Sensitivity to Surface Roughness

Sensitivity to isolated roughness elements

- Radeztsky, Reibert, and Saric (1999)
- The model has a pressure minimum on the upper surface at approximately x/c = 0.71
- With a 45-deg sweep and a small negative angle of attack.
- Produces a boundary-layer flow that is subcritical to T-S waves at moderate chord Reynolds numbers, but produces considerable crossflow

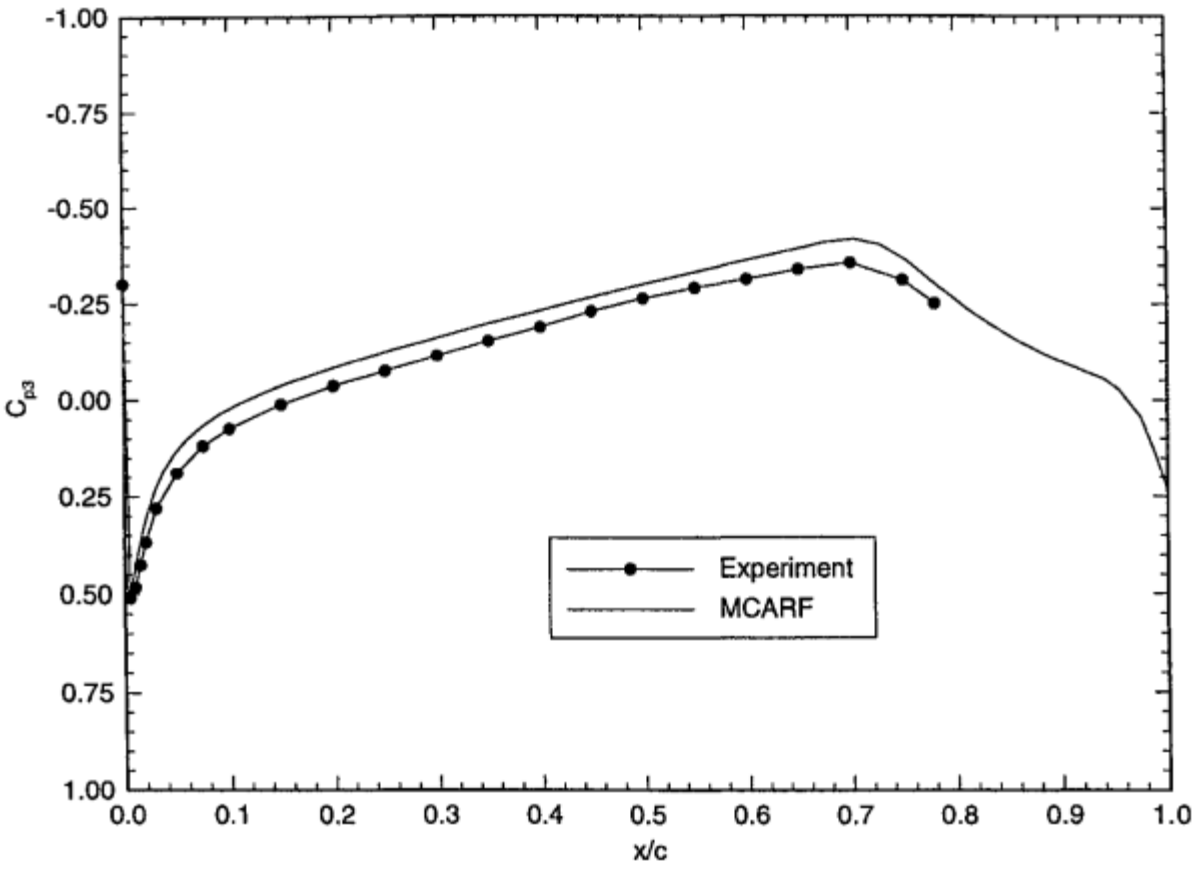

Fig. 1 NLF(2)-0415 upper-surface pressure distribution in wind tunnel at $\alpha = -4$ deg.

Radeztsky, Reibert, and Saric (1999)

Base Surface Roughness

Three base surface roughness levels were tested:

- Painted
- Paint removed, sanded, and machined polished (0.5 um rms)
- Hand polished (0.1-0.25 um rms)

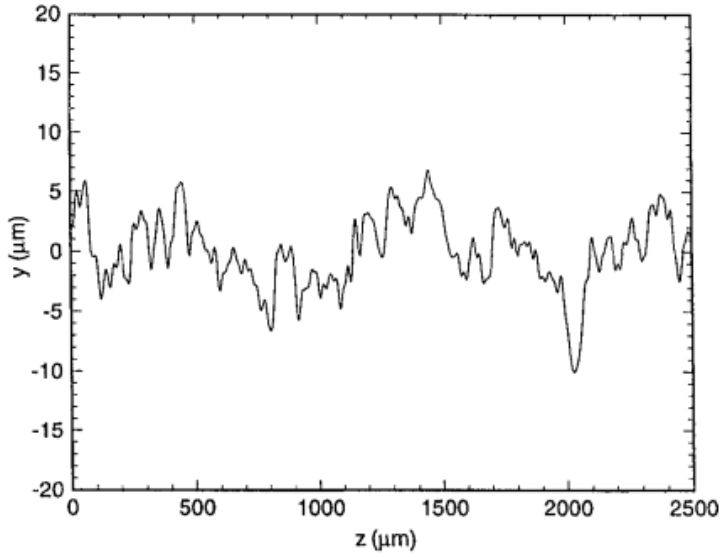

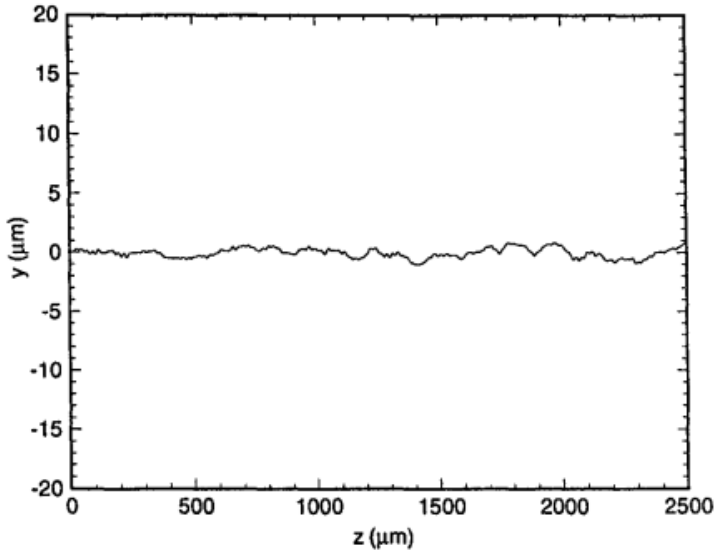

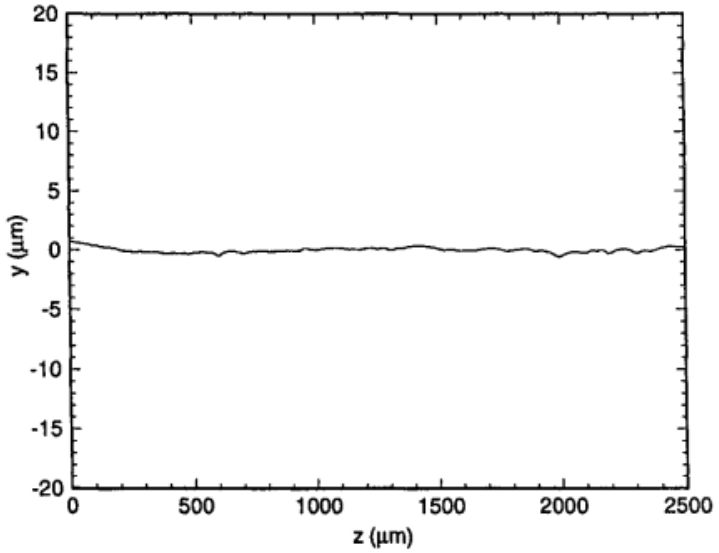

Base Surface Roughness

- Using naphthalene flow visualization, the transition location based on chord Reynolds number was found for all three base roughness conditions
- These results show that the surface finish has a significant effect on the transition location

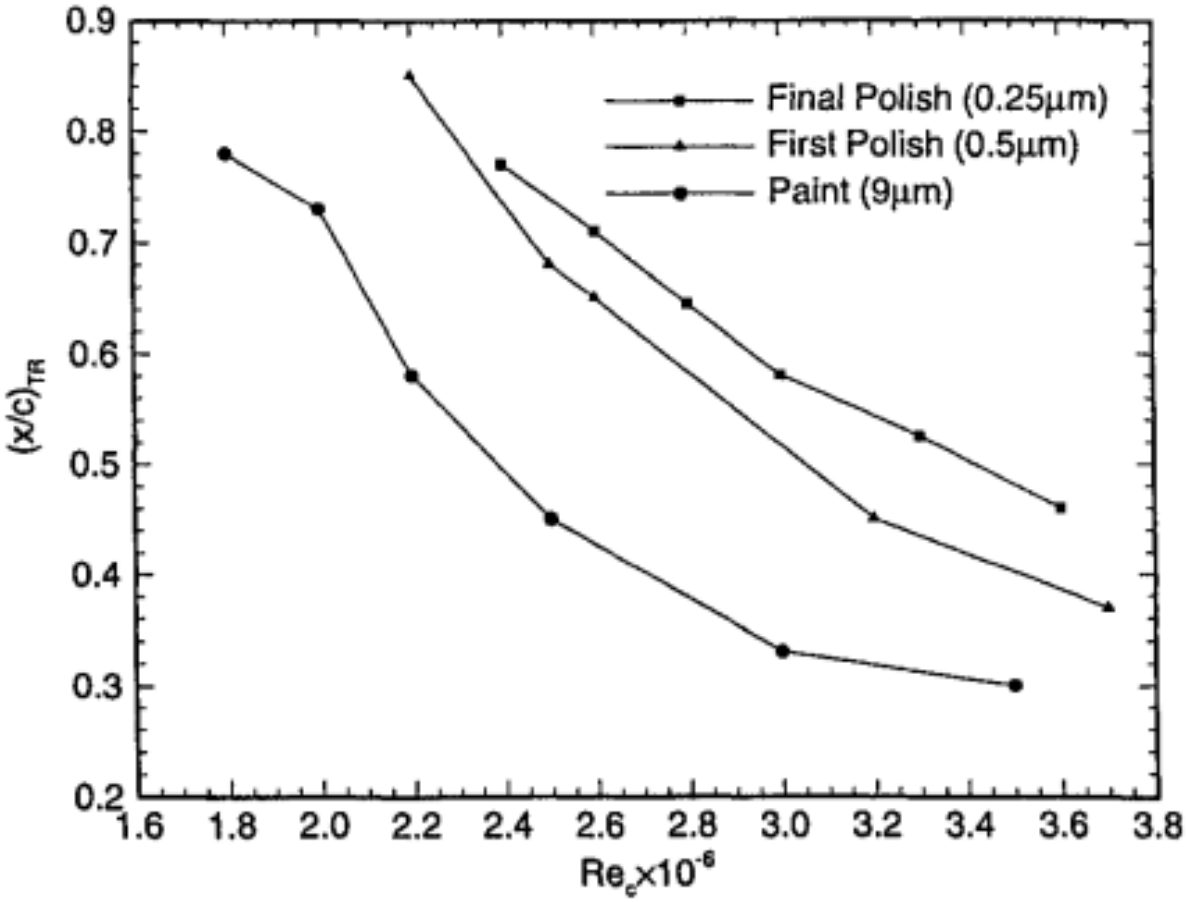

Radeztsky, Reibert, and Saric (1999)

Location of Isolated roughness Element

- Hand polished surface is used
- Roughness element size D = 3.7 mm, H = 6 um
- Important to note that the attachment line is at x/c = 0.007
- Also, the calculated neutral stability point for the most unstable stationary modes is at x/c = 0.02

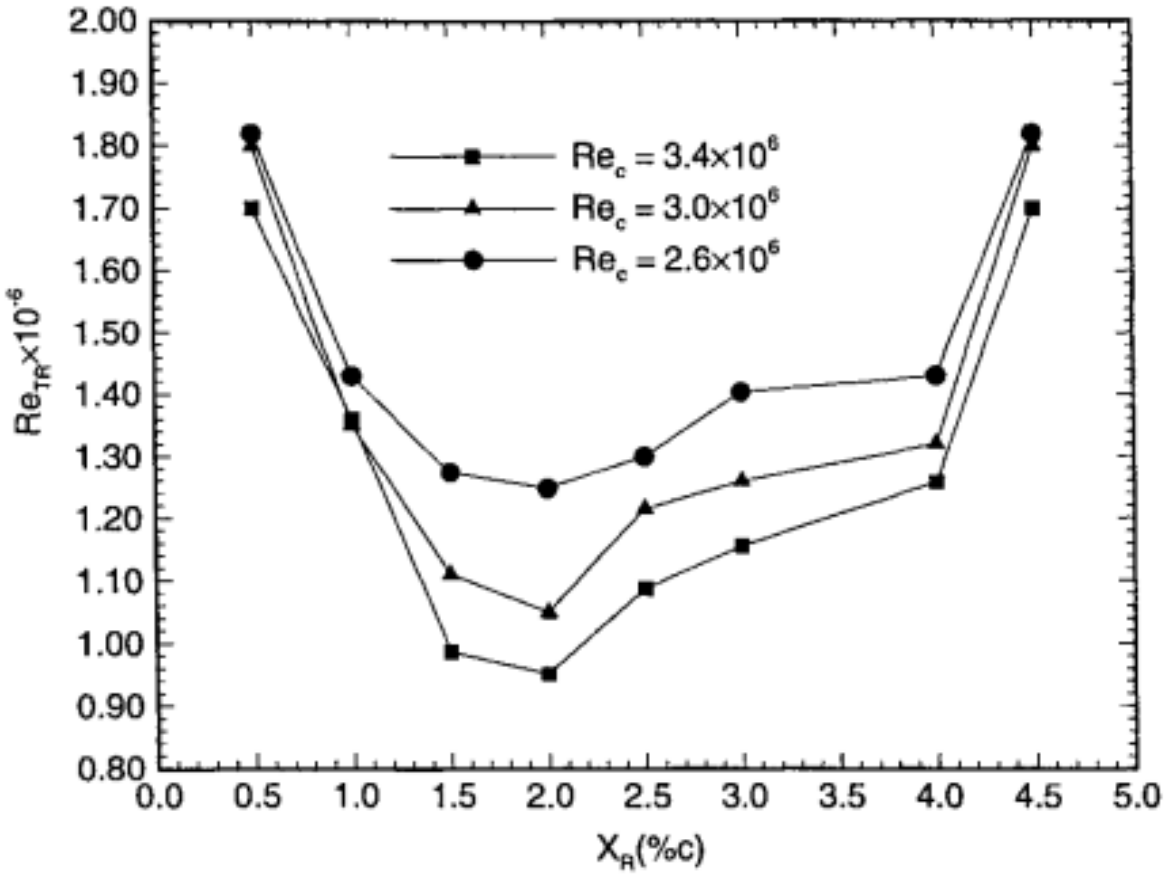

Radeztsky, Reibert, and Saric (1999)

Size of Roughness Element

- (x/c) point for transition is affected by both the roughness element diameter and height
- For the point of smallest diameter, both a height of 6um and a height of 18um were tested but both did not result in transition earlier than that of the unaffected flow

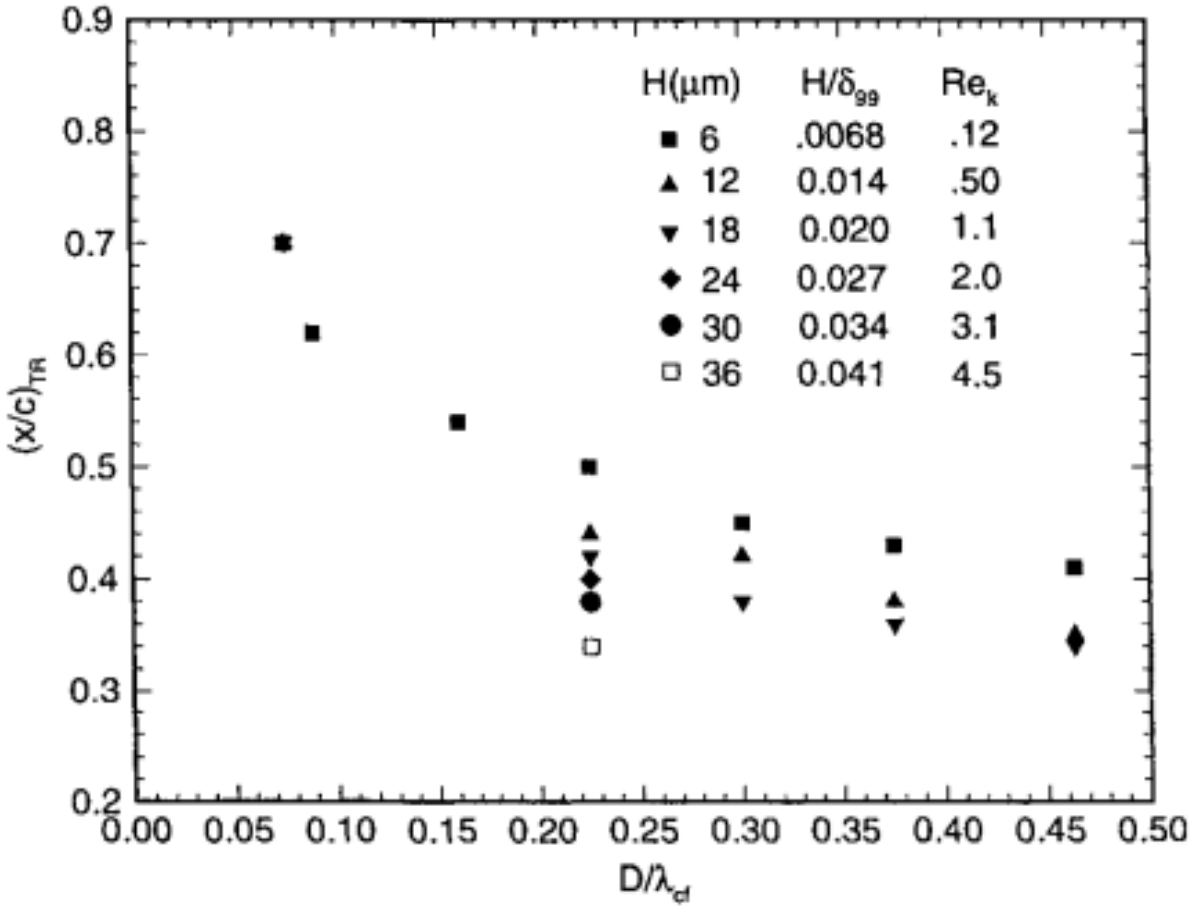

Radeztsky, Reibert, and Saric (1999)

Hot wire scans

- Four different chord locations and three different heights in the boundary layer are chosen for hot-wire scans
- Following the streamline, the isolated roughness element is associated with the spanwise z location of 25mm
- D = 3.7mm, H = 6 um, x/c = 0.023

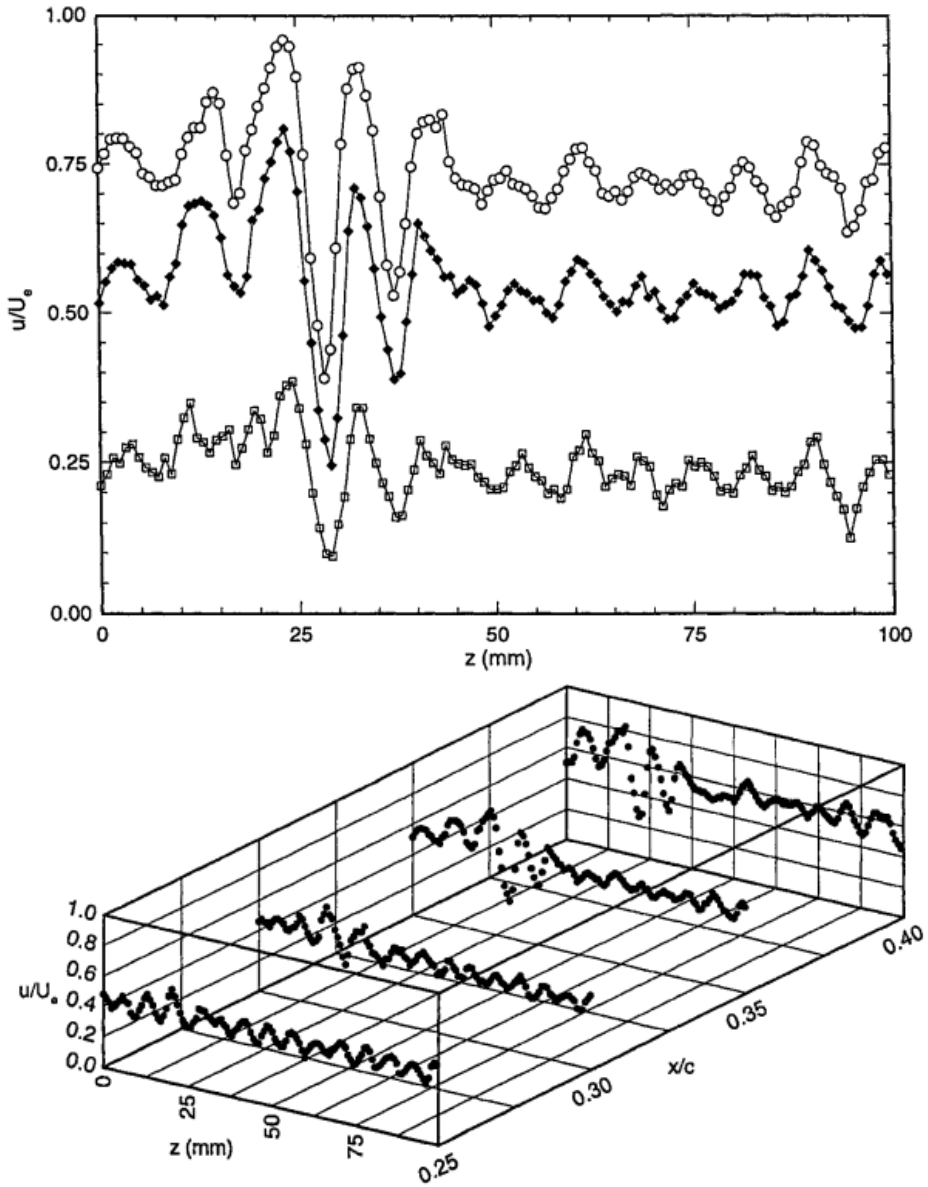

Radeztsky, Reibert, and Saric (1999)

Effect on Wavelength

- Peak is associated with a wavelength of 9.5mm which, when gives the critical wavelength of 8mm when projected in the direction of the crossflow vector
- The addition of a disturbance amplifies the already most unstable frequency
- x/c = 0.4 and u/U = 0.75

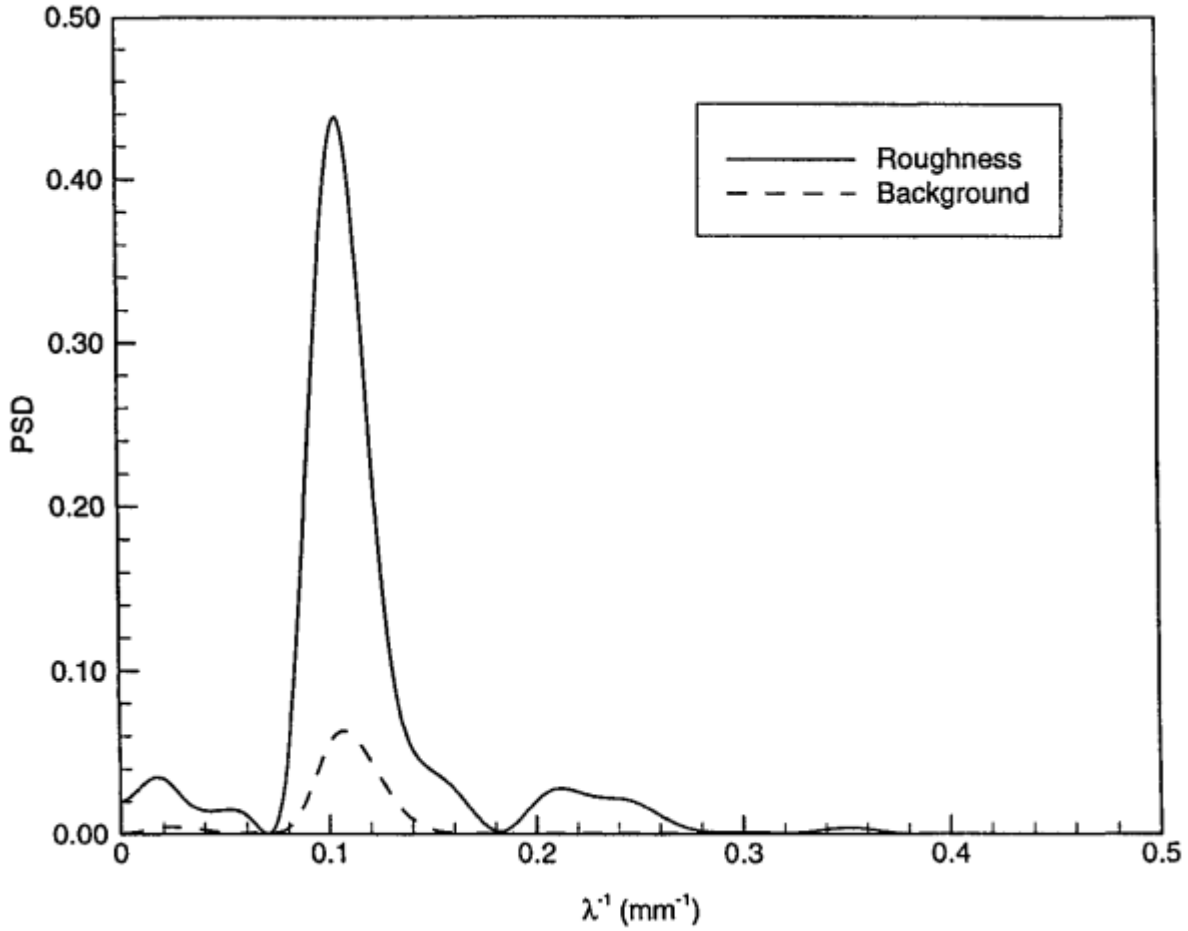

Radeztsky, Reibert, and Saric (1999)

Effect on Critical Wavelength

- Shows the amplification of the critical wavelength is increased with the addition of a roughness element

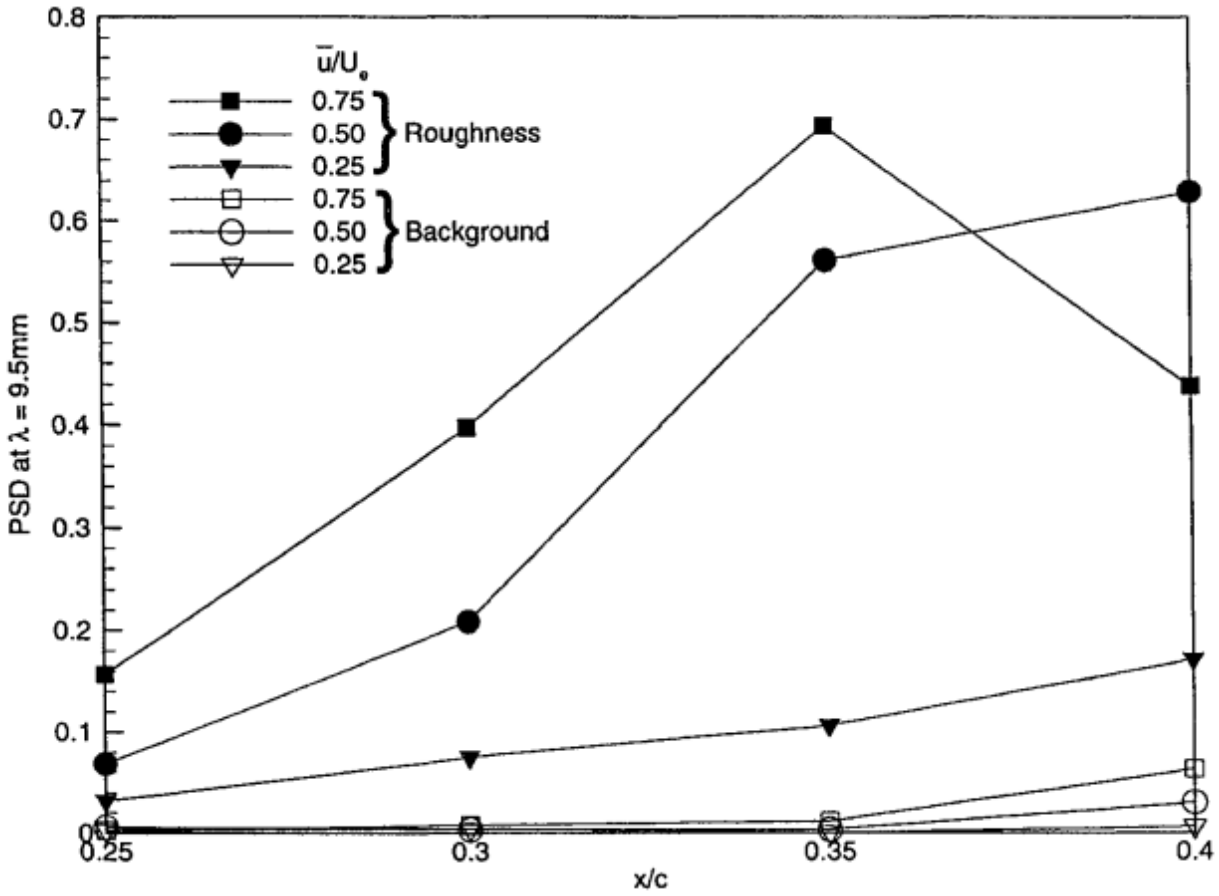

Radeztsky, Reibert, and Saric (1999)

Transition to Turbulence

Transition to Turbulence

- Wassermann and Kloker (2002)
- Sought to understand the secondary instability and how to delay the onset of turbulence
- Performed a numerical study on the system shown here

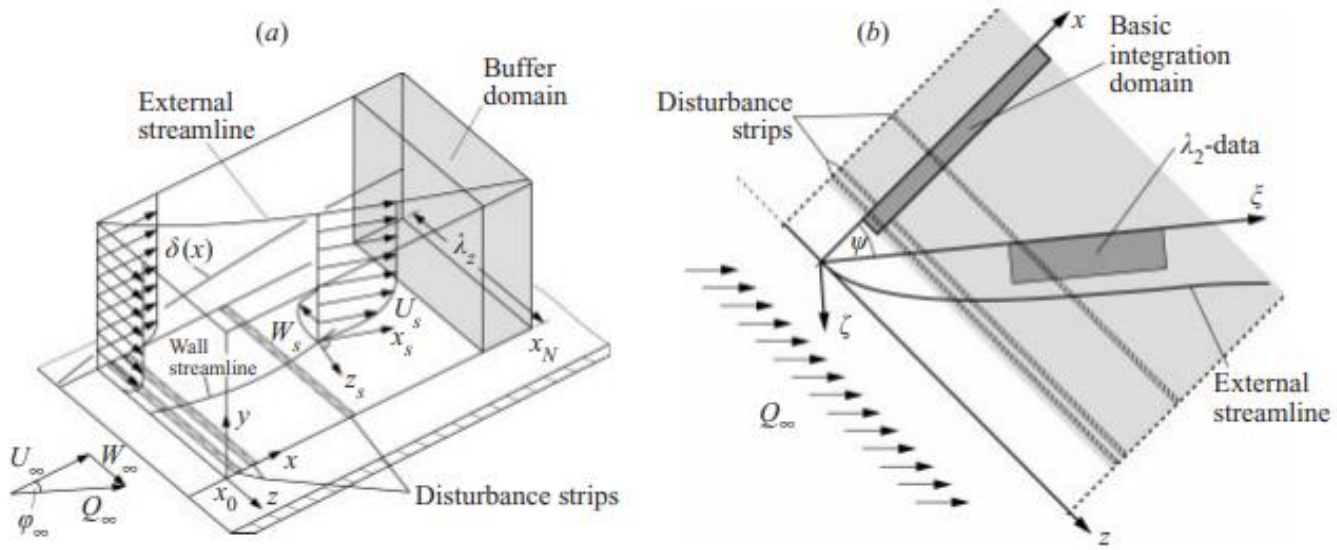

FIGURE 1. (*a*) Integration box. (*b*) Top view of the swept flat plate with the vortex-oriented coordinate system ((ξ, ζ), rotated by $\psi = 39°$ versus the chordwise system).

Wassermann and Kloker (2002)

Characteristics of the Baseflow

- The laminar base flow was designed to resemble the flow in the front region on a swept wing. Taken from Spalart et al. (1994)
- The spanwise component relative to the chordwise component of the velocity decreases

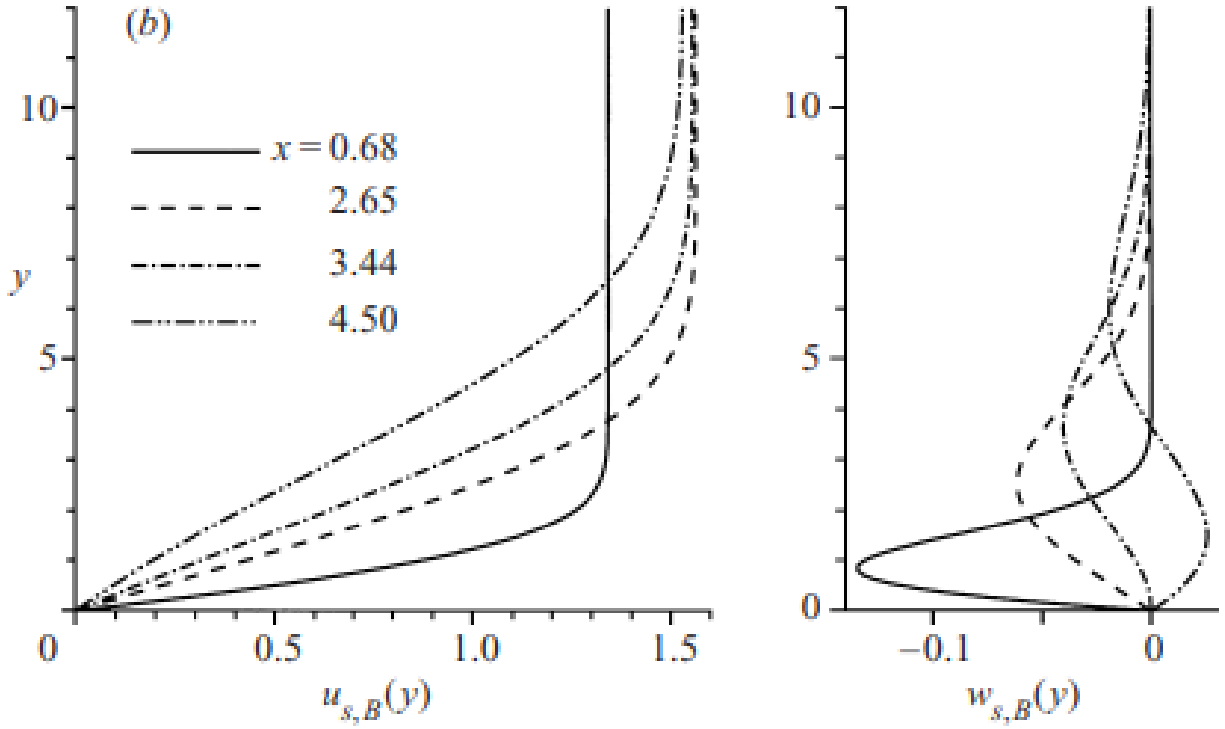

Wassermann and Kloker (2002)

Stability Diagram

- For steady crossflow vortices from LST.
- LST analysis was done using the special model. $\alpha_i = 0$ forms the neutral loop
- The fundamental spanwise wavenumber was chosen to be $\gamma_1 = 45$

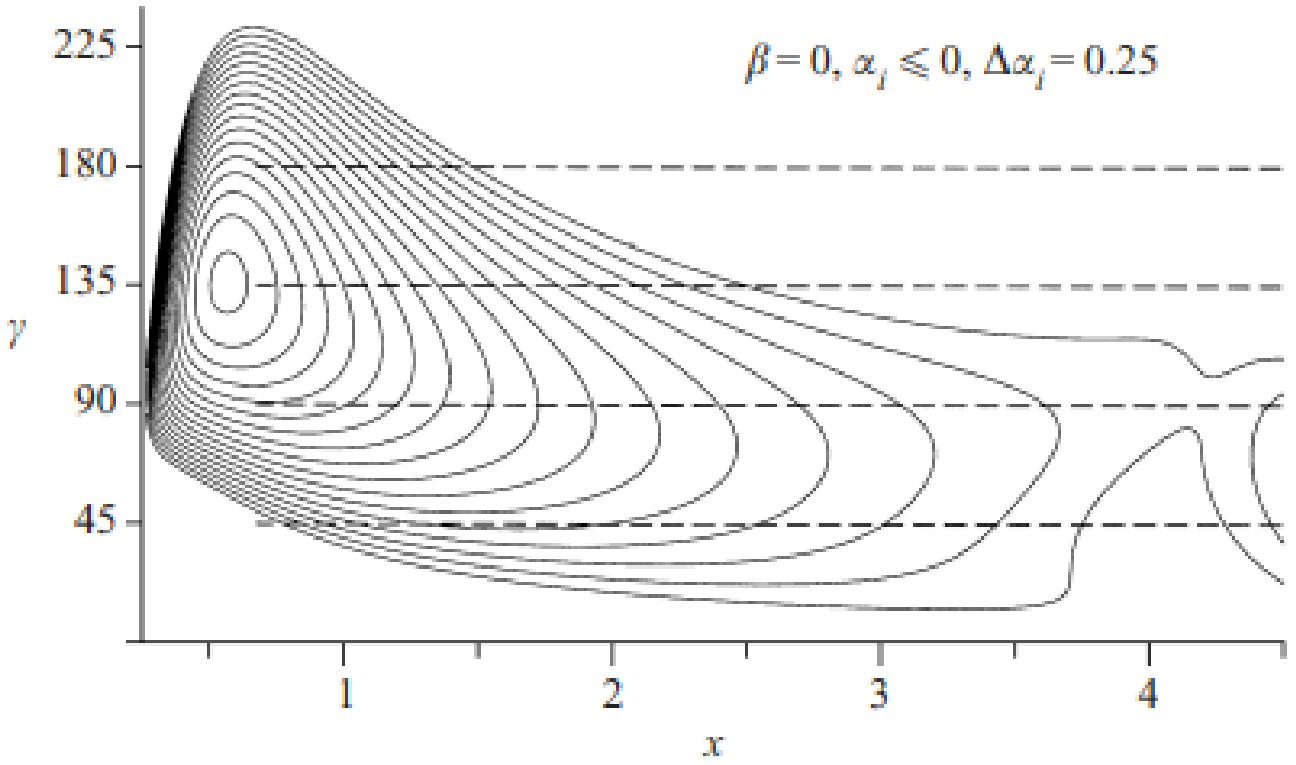

Wassermann and Kloker (2002)

Amplitude Development

- Downstream amplitude development of the crossflow vortex packet
- Notation (h,k) where h is the frequency and k is the spanwise wavenumber k*γ1.
- Note that here (0,2) mode is dominant and eventually suppresses the growth of the other modes

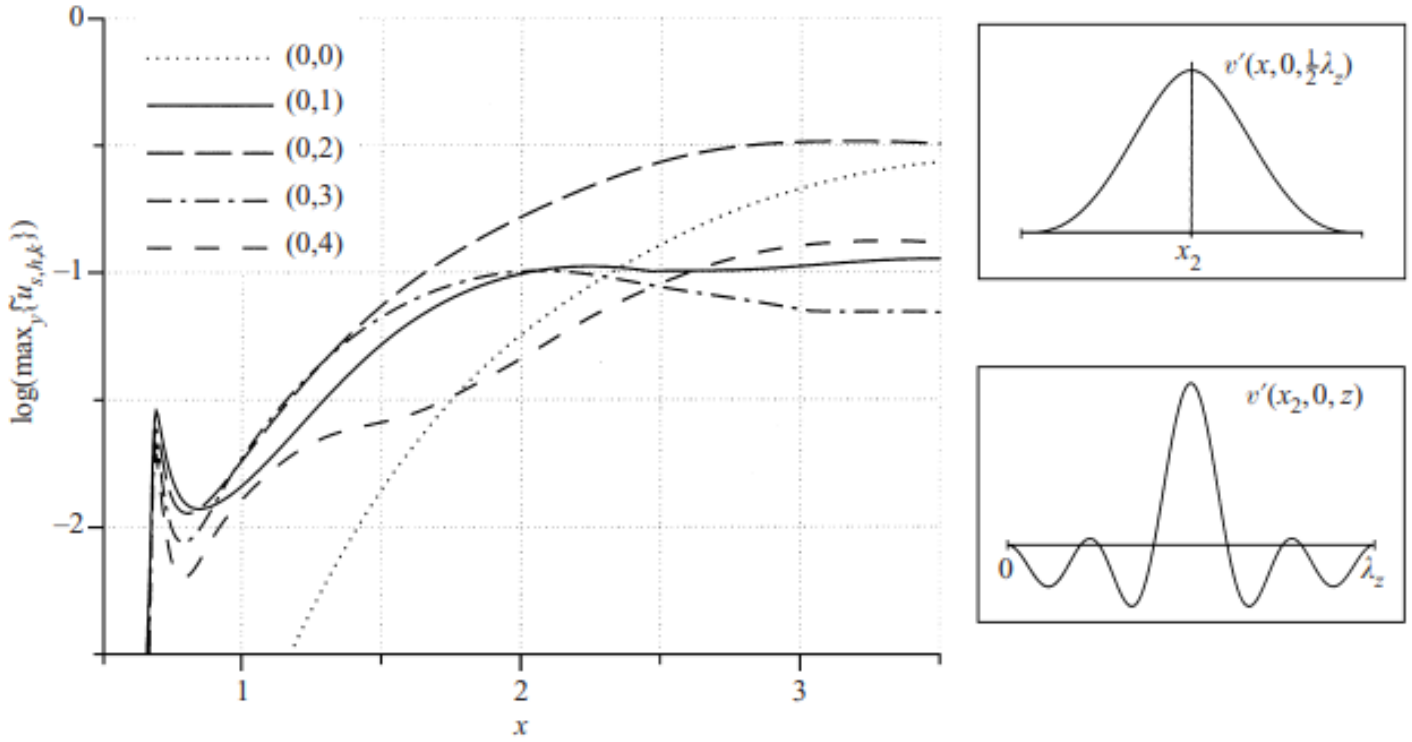

Wassermann and Kloker (2002)

Flow Field Distortion

- Distortion to the flow field by nonlinearly saturated crossflow-vortex-mode packet
- Notice second vortex that forms in the up-welling region. This weak vortex is considered to have small relevance

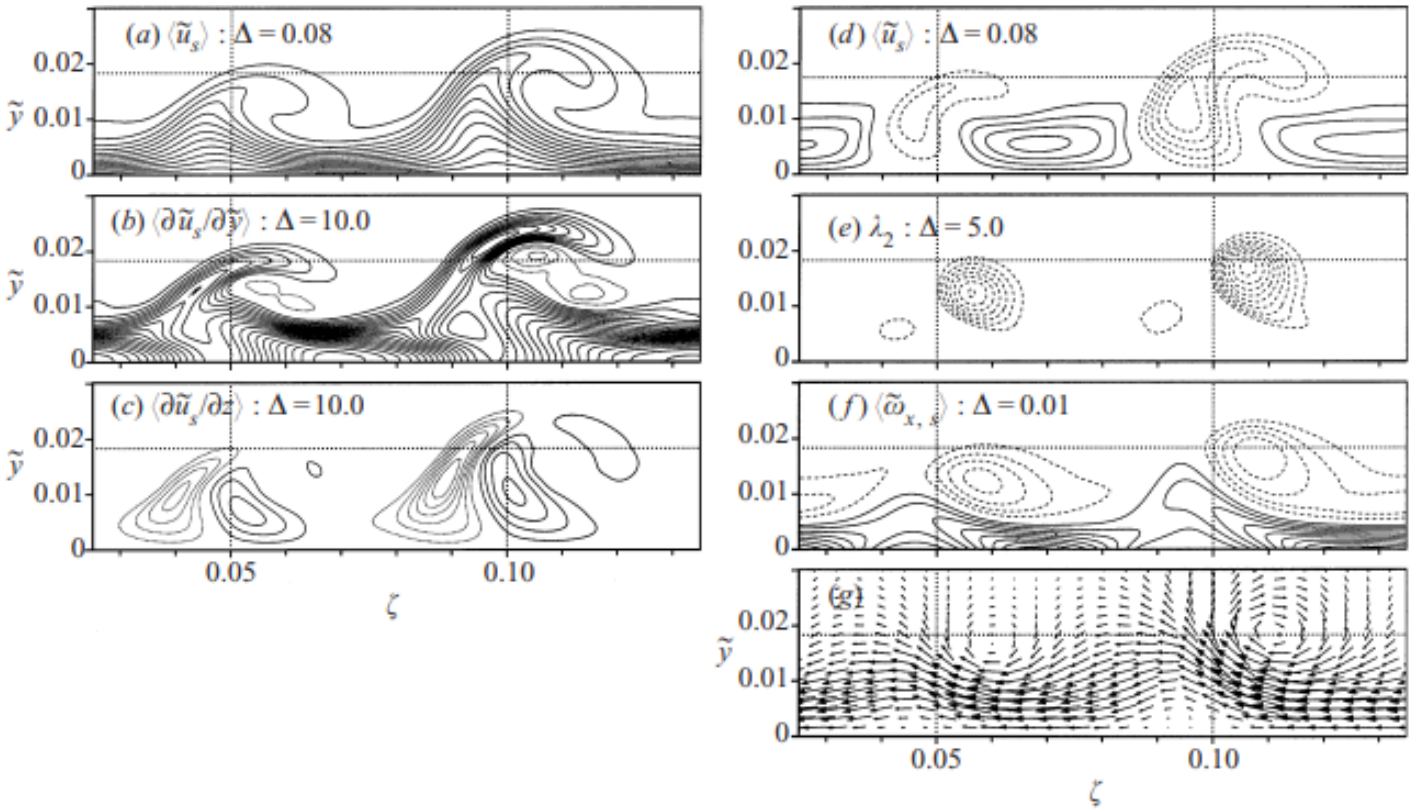

Wassermann and Kloker (2002)

Periodic Background Pulses

- Previously only a steady disturbance has been discussed but to get transition to turbulence, an unsteady disturbance must be added.
- Periodically pulsed low-amplitude disturbances are added to simulate the natural disturbance background

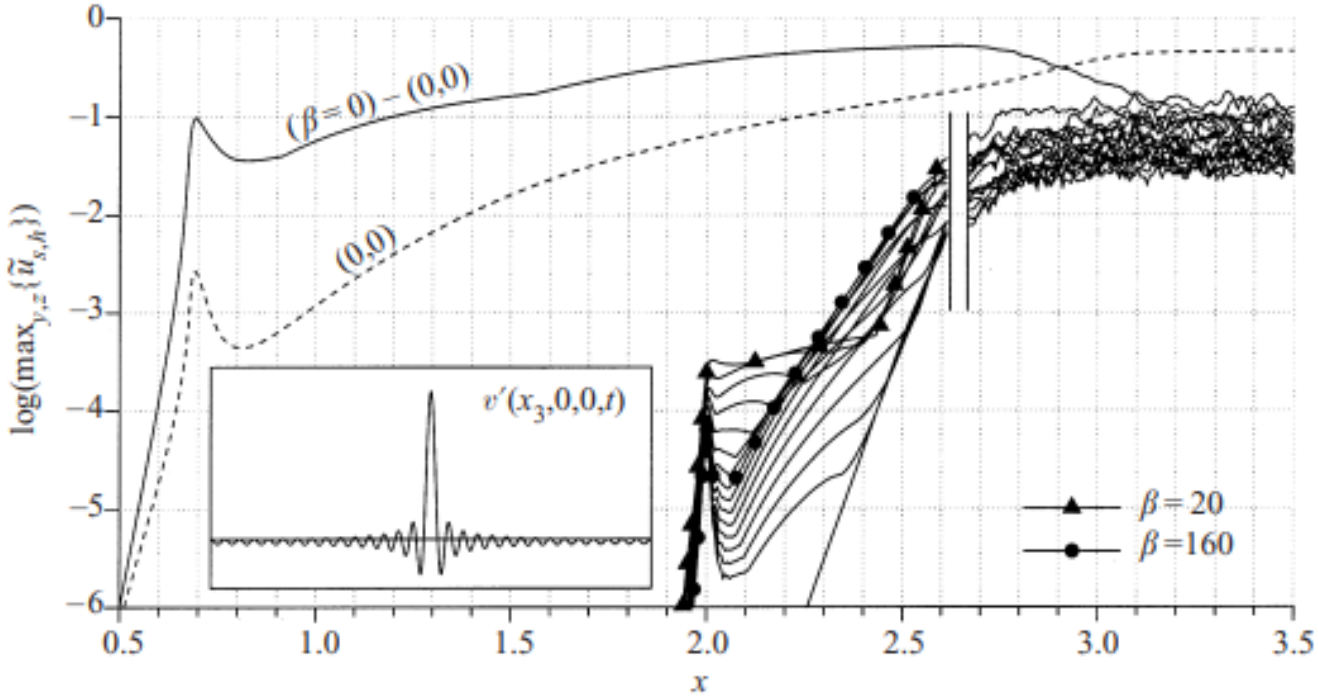

Wassermann and Kloker (2002)

Periodic Background Pulses

- Contours of normalized amplitude for unsteady disturbances
- (a) β = 20 (low frequency)
- (b) β = 160 (high frequency)

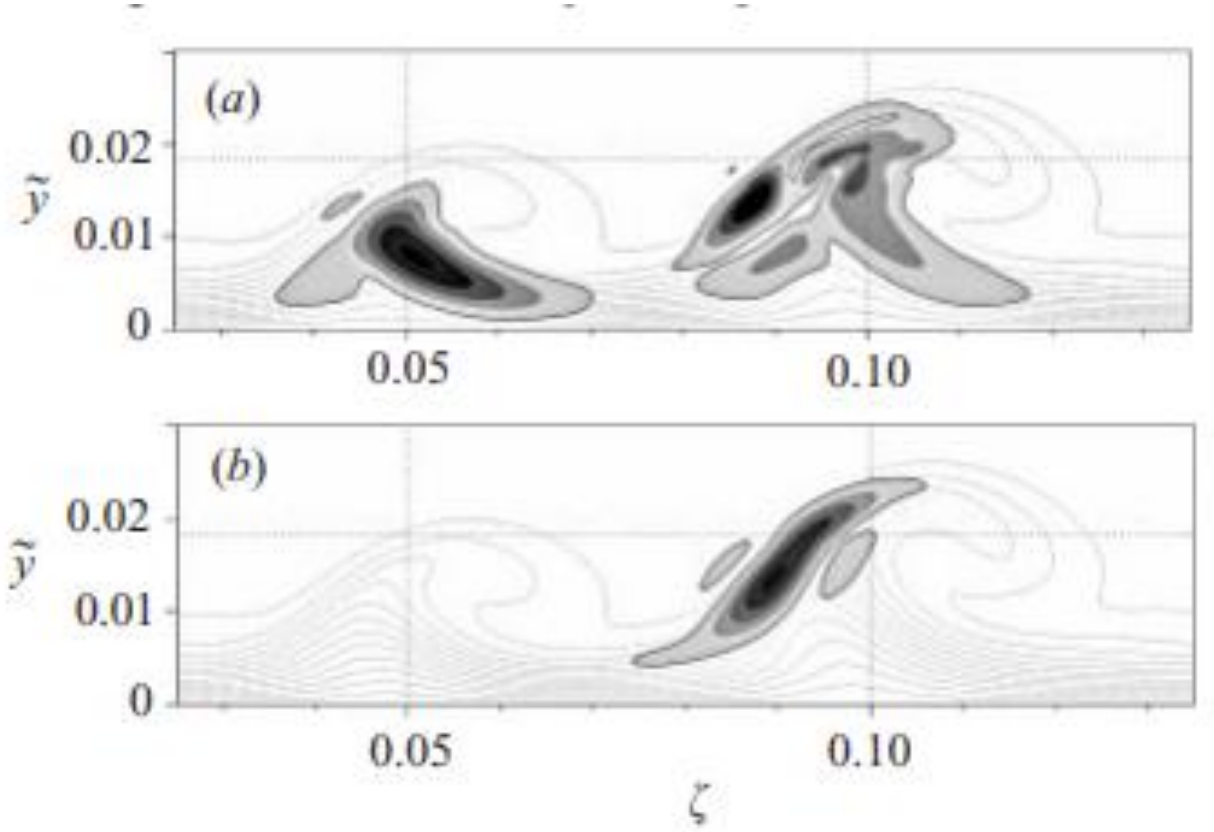

Wassermann and Kloker (2002)

Visualization of Vortex Formation

- Shows the formation of the secondary instability
- From (a) to (d): t/T = 0.5, 0.75, 0, 0.25; T is the period of the background pulses

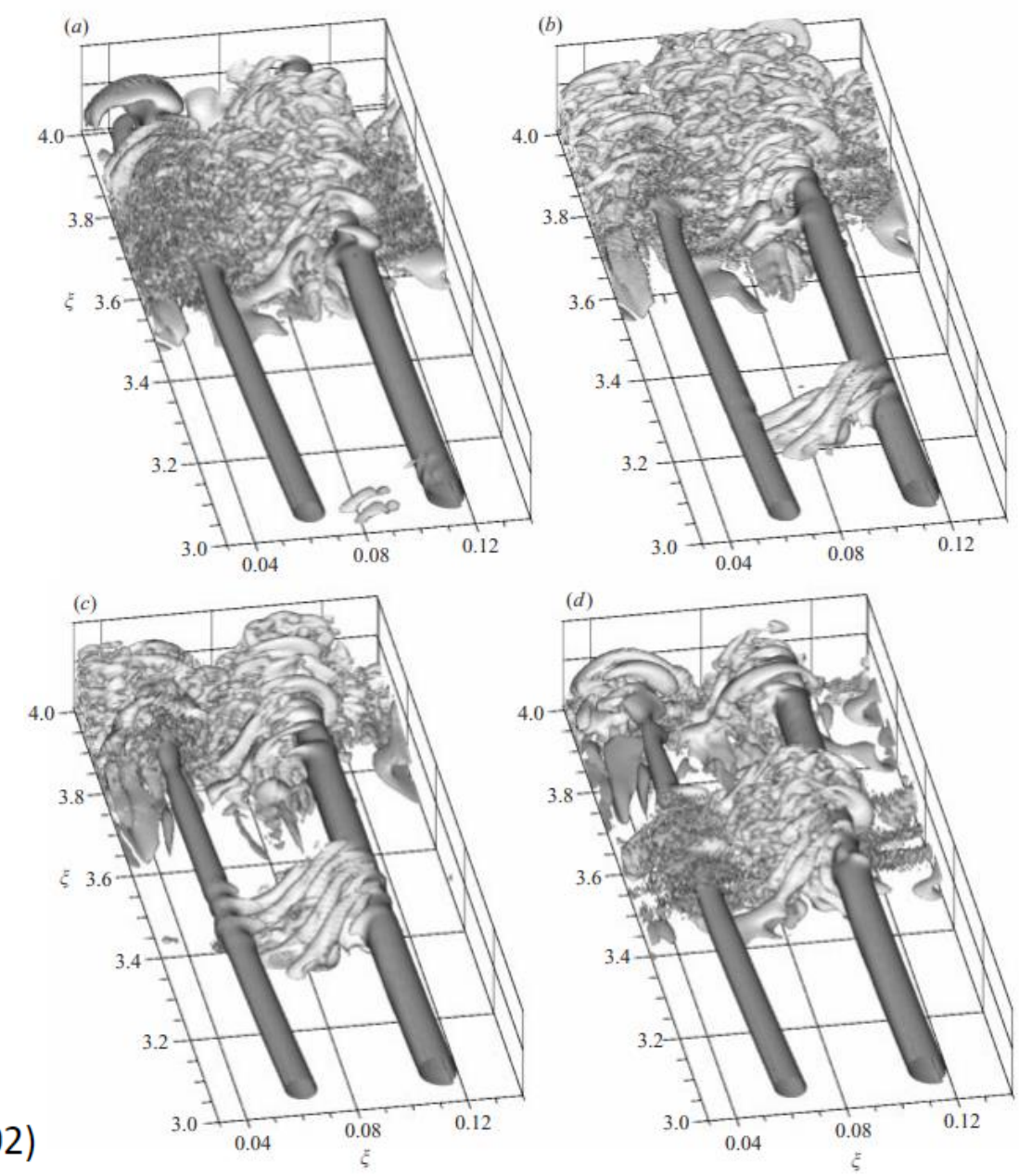

Wassermann and Kloker (2002)

Convective Nature of Secondary Instability

- Crossflow-vortex-mode packet plus periodic background pulses.
- The background pulses are turned off at $t = t_0$.
- From (a) to (d): $t/T = t_0 + 0.85T$, $t_0 + 1.45T$, $t_0 + 2.05T$, $t_0 + 2.65T$

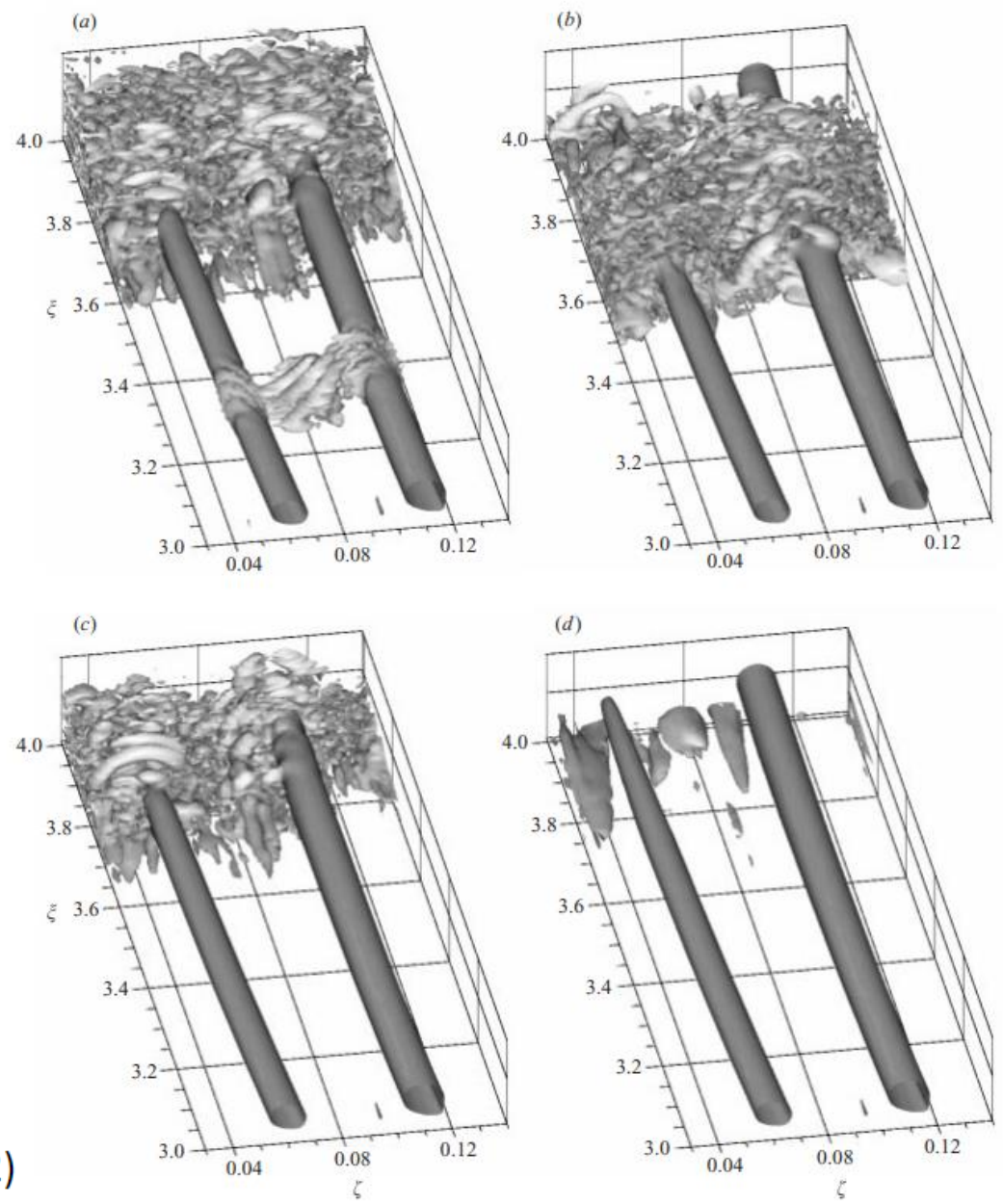

Wassermann and Kloker (2002)

Flight Testing

Experiment Setup

- Saric, Reed, and Banks (2003)
- IR camera was used to visualize flow transition
- Downwash from F-15 was more invasive than expected. Sweep angle of the flow varies from 35 degrees at the base to 30 degrees in the outboard region

Theoretical Amplification

- Legend on both charts is cut off, however the paper reports that the most unstable crossflow vortices had a wavelength of 4mm (in both the midspan and outboard regions)

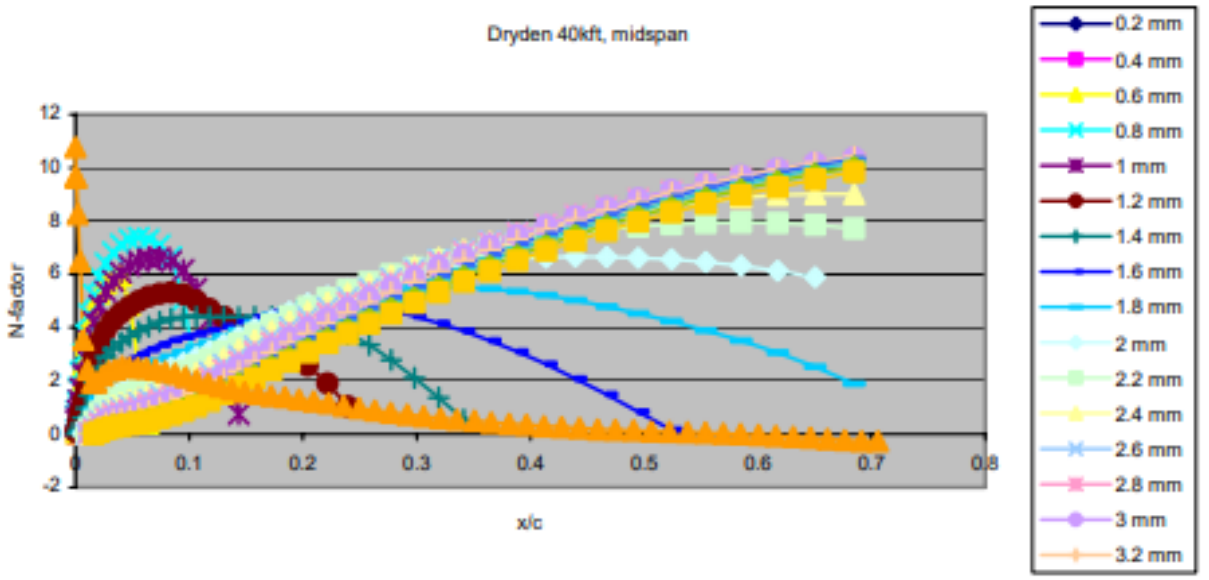

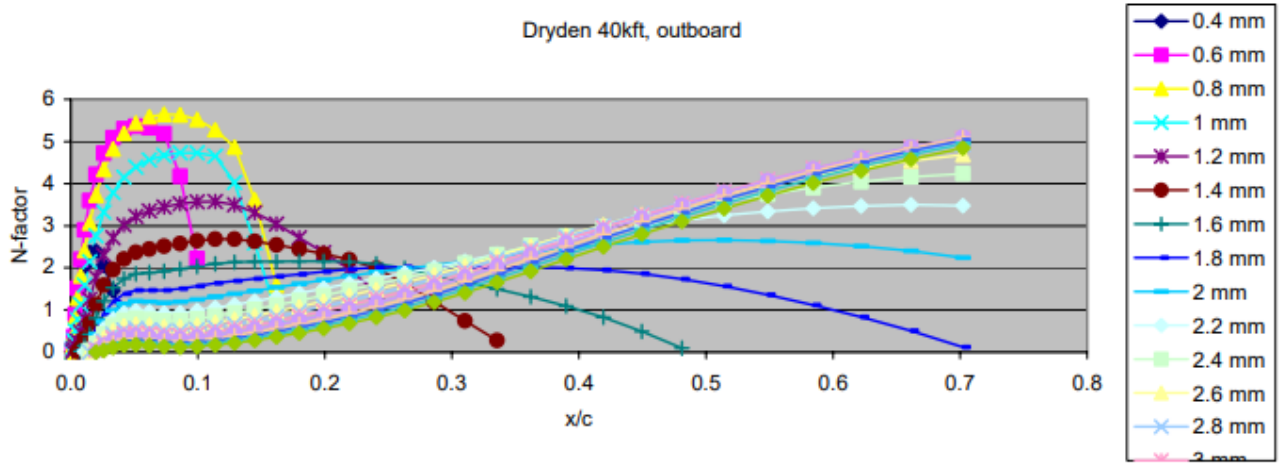

Subsonic Flight Test

- Roughness elements placed 2mm apart
- In this case, flight speed is at Mach 0.911
- Nearly full cord laminar flow
- In this case dark regions show turbulence

Supersonic Flight Test

- Mach 1.85
- There was a higher-than-expected suction peak and inboard sweep angle made the inboard flow control useless
- In this case the lighter regions show turbulence

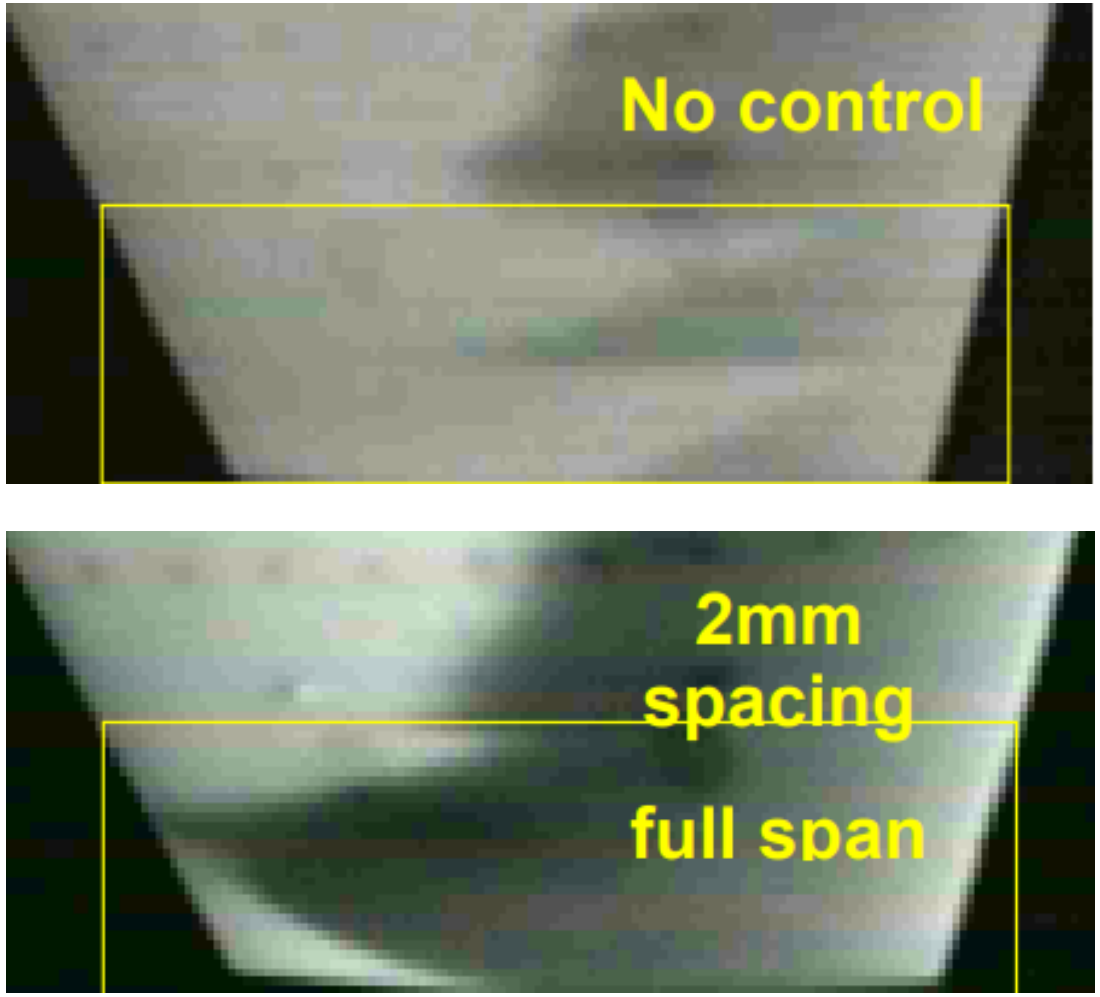

Summary

- The crossflow instabillity is highly sensitive to surface roughness
- The secondary instability is caused by disturbances in the free stream and are most heavily amplified in the low momentum region of the flow field
- Distributed roughness elements can delay the transition to turbulance in subsonic and supersonic flows

Questions?

Sources

- Meersman M. 2021. Free-flight Experiments on Swept Laminar Separation Bubbles
- Radeztsky RH Jr, Reibert MS, Saric WS. 1999. Effect of isolated micron-sized roughness on transition in swept-wing flows
- Reed HL, Saric WS. 1989. Annual Review of Fluid Mechanics
- Reibert MS. 1996. Nonlinear Stability, Saturation, and Transition in Crossflow-dominated Boundary Layers
- Saric WS, Reed HL, White EB. 2003. Annual Review of Fluid Mechanics
- Saric WS, Reed HL, Banks DW. 2003. Flight Testing of Laminar Flow Control in High-Speed Boundary Layers
- Serpieri J. 2018. Cross-Flow Instability, Flow diagnostics and control of swept wing boundary layers
- Wassermann P, Kloker M. 2002. Mechanisms and control of crossflow-vortex induced transition in a 3-D boundary layer